Proceedings of the 2nd International IEEE EMBS
Conference on Neural Engineering
Arlington, Virginia · March 16 - 19, 2005

Design of a Wideband Power-Efficient Inductive Wireless Link for Implantable Biomedical Devices Using Multiple Carriers

Suresh Atluri[1] and Maysam Ghovanloo[1,2]

[1]Department of Electrical and Computer Engineering, [2]Department of Biomedical Engineering,
North Carolina State University, Raleigh, NC, USA

Abstract— **This paper presents a novel design for wireless transmission of power and bidirectional data to biomedical implantable microelectronic devices using multiple carrier frequencies. Two separate pairs of coils have been utilized for inductive power and forward data transmission. A back telemetry link is established with a pair of patch antennas in the Industrial-Scientific-Medical (ISM) band. Achieving high power transmission efficiency and high data transmission bandwidth with minimum Bit Error Rate (BER) are the main goals in this application. One of the major challenges is to minimize the interference among carriers especially on the implantable side, where size and power are highly limited. The planar power coils are spiral shaped, and optimized in size to provide maximum coupling coefficient. The data coils are designed rectangular across the power coils diameter and oriented at right angles to the power coils planes to maximize their direct coupling, while minimize their cross-coupling with the power coils. The power, forward data, and back telemetry carriers, which are orders of magnitude different in amplitude, are widely separated in frequency at 125 kHz, 50 MHz, and 2.45 GHz range to further reduce the interference and facilitate filtering. Robust modulation and encoding techniques are currently under development to minimize the effects of interference even further.**

Keywords—**Biomedical implants, coupling coefficient, data rate, efficiency, frequency shift keying, inductive link, interference, radio frequency, telemetry, wireless**

I. INTRODUCTION

An inductive link between two magnetically-coupled coils is now one of the most common methods to wirelessly transmit power and data from the external world to implantable biomedical devices such as neuromuscular stimulators, cochlear implants, and visual prostheses [1]-[3]. These devices are either battery-less and should be continuously powered from an external portable battery, or have miniature rechargeable batteries that should be inductively charged on a regular basis. In both cases, the inductive power transmission should be very efficient to minimize the size of the external battery, and eliminate overheating of the surrounding tissue by surpassing the exposure limit to electromagnetic field [4].

Neuroprostheses that substitute sensory functions need sizeable amounts of real-time data to interface with a large number of neurons by means of tens to hundreds of stimulating sites that are driven through multiple parallel channels [5]. As a result, wideband data transmission is another requirement for the wireless link. The wireless link should also be robust enough not to be affected by patient's motion artifacts or minor coils misalignments. To achieve this characteristic, a reverse telemetry link is needed for the implant power regulation and data integrity. The back telemetry link can also be used for the stimulating sites impedance measurement *in situ* and recording the neural response to stimulus pulses for accurate electrode placement and stimulation parameter adjustments.

The wireless link operating frequency, also known as carrier frequency, is one of the most important parameters of the implantable biomedical system. Traditionally, a single carrier frequency has been used for (1) inductive power transmission, (2) forward data transmission from the outside world towards the implanted device, and (3) back telemetry from the implanted device outward [1]-[3]. Achieving high power-transmission efficiency, high data-transmission bandwidth, and coupling insensitivity using the traditional single carrier method would be very challenging, if not impossible, because of the conflicting constraints that are involved in achieving high performance in two or more of the above system requirements. For example, increasing the carrier frequency can result in wider bandwidth for forward data transmission. However, it degrades power transmission efficiency due to more power absorption/deposition in the tissue and more power dissipation in the external and internal power conditioning blocks. In addition, using the same carrier for back telemetry by switching the load across the implanted receiver coil, known as load shift keying (LSK), also hinders the power transmission efficiency by affecting the receiver coil quality factor, Q, and the data rate is limited to tens of kilo-bits-per-second (kb/s) [1].

The solution that we propose in this paper in order to achieve a high performance in all of the aforementioned system requirements is to utilize three carrier signals at three different frequencies and amplitude levels, which are optimal for the above three major wireless link functions, to effectively isolate many of the competing parameters in the design of a wireless link: (1) low-frequency (f_P < 1 MHz) high-amplitude carrier for power transmission, (2) medium-frequency (f_{FD} = 25~50 MHz) medium-amplitude for forward data transmission, and (3) high-frequency (f_{BT} > 1 GHz) low-amplitude for back telemetry. Fig. 1 shows a functional block diagram of an implantable neuroprosthesis system with multiple carrier frequencies.

The main challenge in using multiple simultaneous carrier frequencies for data and power transmission is the interference

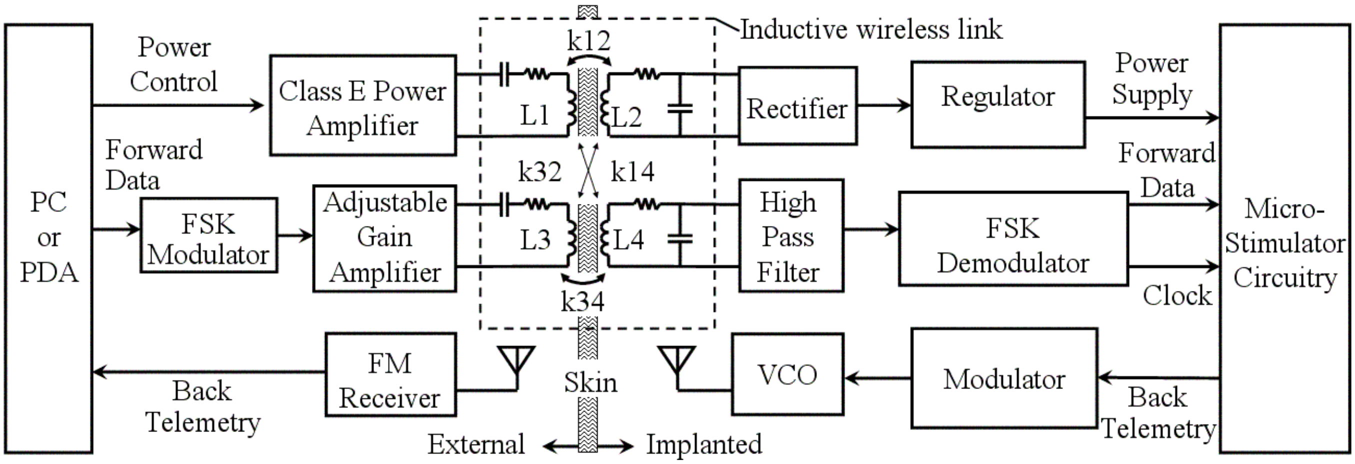

Fig.1. Block diagram of the wireless microstimulating-recording system. The wideband power-efficient inductive wireless link, which is the focus of this paper, is enclosed in a dashed box.

problem. The most difficult part of this problem is eliminating the strong power carrier interference with forward data carrier on the implantable receiver side, where the power budget and size are extremely limited. To address this issue, the following measures are adopted:

1- Two individual pairs of coils are dedicated to power and forward data transmission. The geometry and orientation of the coils are designed in order to occupy a small space, maximize direct coupling within each pair, and minimize cross coupling between the pairs.
2- The data carrier is frequency shift keyed (FSK) [6], to be insensitive to amplitude variations, as opposed to amplitude shift keying (ASK), which is the method that is used in most similar applications [1]-[3].
3- f_{FD} is chosen up to 400 times higher than f_P. This would provide enough spacing between the two carriers in the frequency domain to allow separation of data carrier components and reliable detection of the forward data bits with proper tuning, on-chip filtering, and utilization of a novel FSK demodulation technique [6].
4- The forward data carrier amplitude on the transmitter side, A_{FD}, which is normally about 50 times smaller than the power carrier amplitude (A_P), would be adjustable based on the BER. An increase in BER will lead to an increase in A_{FD} to compensate for the effect of an interfering signal or coils misalignments. BER can be continuously monitored on the implant, using cyclic redundancy checking (CRC), and reported to the external system by means of the back telemetry link.

The back telemetry data, which is out of the scope of this paper, will be carried through a weak microwave link in the ISM band, using miniature patch antennas similar to [7]. The reason being that the implant transmitter has to be low power, while the external receiver, which has more relaxed power consumption and size constraints, can be designed to be very selective and sensitive.

The rest of this paper is dedicated to the theory, modeling, and computational results for the geometrical design of the power and forward data transmission coils. We have also done circuit simulations on power and forward data inductive-capacitive (LC) tank circuits using direct and cross coupling coefficients extracted from the coil models.

II. Self and Mutual Inductanc Equations

In general, the coupling coefficient, k, between two inductively coupled coils, L_1 and L_2, is defined as

$$k = \frac{M_{12}}{\sqrt{L_1 \times L_2}} \tag{1}$$

M_{12}, the mutual inductance of two circular coils with radii R_1, R_2, distance d, and lateral misalignment ρ is [8]

$$M_{12} = \mu_0 \pi \sqrt{R_1 R_2} \int_0^{\infty} J_1\left(x\sqrt{\frac{R_1}{R_2}}\right) J_1\left(x\sqrt{\frac{R_2}{R_1}}\right) J_0\left(x\frac{\rho}{\sqrt{R_1 R_2}}\right) . \exp\left(-x\frac{d}{\sqrt{R_1 R_2}}\right) dx \tag{2}$$

where J_0 and J_1 are the Bessel functions of the zeroth and first order, respectively. For the case of perfect alignment, i.e. when $\rho=0$, (2) simplifies to

$$M = \mu_0 \sqrt{R_1 R_2}\left[\left(\frac{2}{s} - s\right)K(s) - \frac{2}{s}E(s)\right] \tag{3}$$

where

$$s = \sqrt{\left(\frac{4R_1R_2}{(R_1+R_2)^2 + d^2}\right)} \tag{4}$$

$K(s)$ and $E(s)$ are the complete elliptic integrals of the first and second kind, respectively.

According to [8], for the condition of $r/R_1 << 1$, where r is the radius of the wire, the self inductance of a circular loop is approximately

$$L(R_1, r) = \mu_0 R_1 \left(\ln\left(\frac{8R_1}{r}\right) - 2 \right) \quad (5)$$

For the case of circular coils with N turns, the self-inductance is approximately equal to the self-inductance derived in (5), multiplied by N^2. Whereas, for the case of spiral coils having N turns with different radii R_{1i} ($i = 1,2,...N$) the overall self-inductance should be calculated from

$$L = \sum_{i=1}^{N} L(R_{1i}, r) + \sum_{i=1}^{i=N} \sum_{j=1}^{j=N} M(R_{1i}, R_{1j}, \rho = 0, d = 0)(1 - \alpha_{i,j})$$

(6)

where $\alpha_{i,j} = 1$ if $i = j$, and $\alpha_{i,j} = 0$ otherwise [8].

III. Inductive Link Design

We have developed a MATLAB code to model multiple coupled rectangular, circular, and spiral coils by generating the coordinates of the coils for FastHenry-2 [9]. FastHenry-2 is an inductance analysis program capable of computing frequency-dependant self and mutual inductances, as well as parasitic resistances of generic three-dimensional conductive structures. As mentioned in section I, in these models our goal is to find the parameters that have the most significant effect in maximizing direct coupling between the two power coils or the two data coils, while minimizing the cross coupling between these pairs.

A. Power Coils

The following notation is adopted from [8] to describe the spiral coils: Coil '**L**' is described as $\mathbf{L} = [R_{max} : -\Delta : R_{min}]$, where R_{max} is the outer radius, R_{min} is the inner radius, and Δ is the spacing between every two adjacent turns of the coil. Obviously Δ should always be greater than the diameter of the wire, $2r$. The number of turns in a spiral coil can be calculated by

$$N = \frac{R_{max} - R_{min}}{\Delta} + 1 \quad (7)$$

The theoretical equations in section II, suggest that the coupling coefficient should not be a strong function of N in ideal circular coils since by increasing N both numerator and denominator of (1) increase at almost the same rate. To observe the effect of N on the coupling coefficient between two identical spiral coils separated by d = 5 mm, we kept R_{max} constant equal to 10 mm and added new turns towards the center of the coil by decreasing R_{min}. Fig. 2 illustrates how k changes as a function of N when Δ = 0.3 mm and $r \approx 0.1$ mm. It can be seen that the highest k can be achieved with N = 23, which is corresponding to R_{min}/R_{max} = 0.34. This is in agreement with $R_{min}/R_{max} \approx 0.4$ in [8].

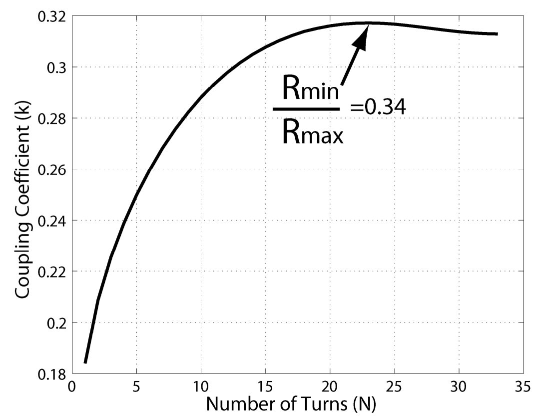

Fig. 2. To maximize the coupling coefficient, k, between two identical spiral coils, R_{max} the outer radius, R_{min} the inner radius, Δ the spacing between two adjacent turns, and N the number of turns should be selected such that R_{min}/R_{max} = 0.34.

Another important design parameter that can affect k is the outer diameter of the primary (external) and secondary (implanted) coils with respect to their distance. According to (3) increasing R_1 and R_2 equally help in increasing M. However, there is a size constraint over R_2, which is imposed by the maximum allowable size of the implant. Therefore, the first guideline is to choose R_2 (R_{2max} in spiral coils) as large as the implant size allows.

To find the best R_1, we limited R_2 to 10 mm and changed R_1 from 8.5 mm to 13.5 mm for d = 5, 6, 7, and 8 mm. Fig. 3a shows that as distance d increases there is an optimum value for R_1, which maximizes k. A similar set of models were set up for a pair of spiral coils, $\mathbf{L_1} = [R_{1max} : -\Delta : R_{1min}]$ and $\mathbf{L_2} = [R_{2max} : -\Delta : R_{2min}]$, with R_{2max} kept constant at 10 mm, while varying R_{1max} from 8 mm to 24 mm for different values of d. Fig. 3b shows that the optimal R_{1max} is larger and changes in a wider range for the spiral coils compared to the single turn coils. It should also be noted that the k values are more than twice larger.

B. Data Coils

The secondary power coil, L_2 with the radius R_{2max}, was chosen to indicate the implant outer perimeter (not to consider packaging). Therefore, the receiver data coil, L_4, should be implemented within the same space. We chose L_4 coil to be rectangular in shape and wound across the diameter of L_2 to give it the maximum possible length $l_4 \approx 2R_{2max}$ (see Fig. 5). The external data coil, L_3, was chosen with the same shape to achieve a fair coupling between two parallel wires. Fig. 4a illustrates the variation of k between two identical rectangular coils when one coil is rotated from 0 degrees in parallel to the second coil (position A) by 90º. The coils have minimum k when they are at right angle (position B). Now keeping the first coil at 90º, the second coil is also rotated from 0 to -90º. It can be seen that k improves when both coils are in the same plane (position C). The rotation is done pivotal to one side of each coil such that the original vertical distance between the coils is not changed.

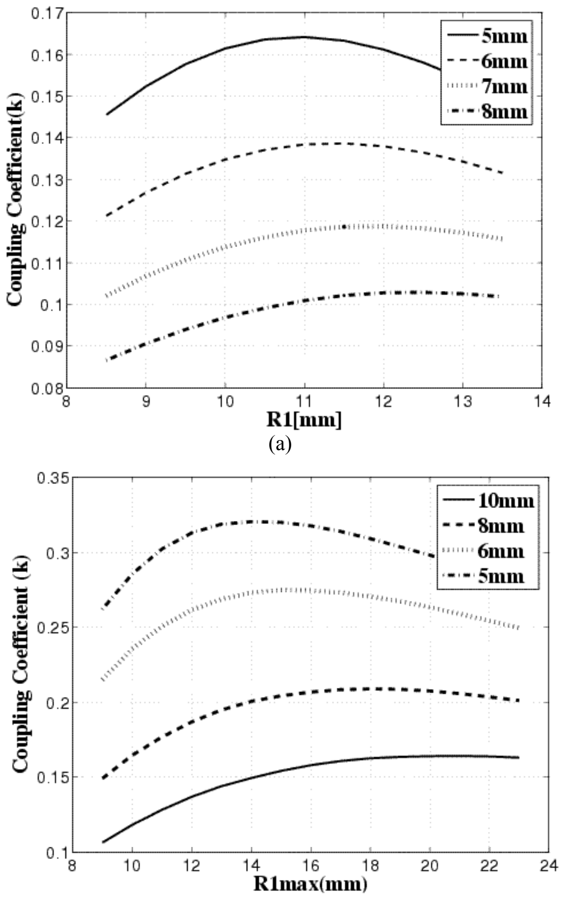

(a)

(b)

Fig. 3. (a) Coupling coefficient between to circular coils with radii R_1, and R_2 = 10 mm as a function of R_1 and distance, d, between the coils (b) Similar settings for two spiral coils with R_{2max} = 10 mm.

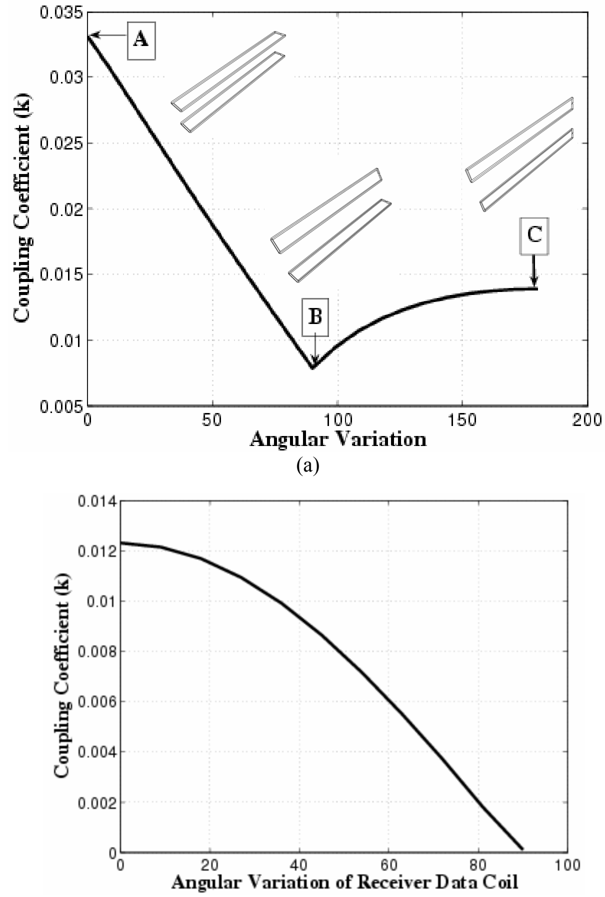

(a)

(b)

Fig. 4. (a) Coupling coefficient between two identical rectangular coils in parallel [A], perpendicular [B], and in the same plane [C] (b) Coupling coefficient between the external spiral power coil and the internal rectangular data coil as it rotates from parallel to perpendicular position.

In a similar setup, Fig. 4b shows the cross coupling coefficient between a spiral power coil and a rectangular data coil at d = 10 mm as the rectangular coil rotates from parallel to perpendicular position with respect to the spiral coil plane. It can be seen that in this case k is almost proportional to $\cos\varphi$, where φ is the angle between the two coil planes.

It can be concluded from Fig. 4 curves that even though parallel rectangular data coils in position A provide higher direct coupling compared to those in the same plane (position C), when considering the cross coupling between each data coil and the two parallel spiral power coils, position C in Fig. 4a would be the best option. This greatly helps reducing the interference between power and forward data carriers, especially on the implant receiver data coil (L_4).

C. Coil Geometries and Orientations

Even though the inductive wireless link in this paper has not been designed for a specific application, an implantable power coil radius of R_{2max} = 10 mm seems to be a reasonable size for ocular, cochlear, and cortical applications [5], [7]. The maximum distance between the power coils is assumed to be about 10 mm. Therefore, from Fig. 3b the optimum radius for the external power coil, R_{1max} = 20 mm. The rectangular primary and secondary data coils, which are wound across the power coil diameters, perpendicular to their planes, are 42 mm × 5 mm and 21 mm × 1 mm, respectively. Fig. 5 shows a rendered 3-D view of the power and forward data transmission coils, and Table 1 summarizes their self inductance as well as direct and cross coupling factors calculated by FastHenry-2. Notice that k_{12}, the direct coupling between power coils is quite large (0.167) and can result in efficiencies higher than 60% [8], [10]. Also note that k_{14}, the cross coupling between the external power and

TABLE I
SELF INDUCTANCE AND COUPLING COEFFICIENTS FOR POWER AND DATA COILS

	L1	L2	L3	L4
L1	59 µH	0.16688	0.00224	0.00012
L2	0.16688	6.55 µH	0.00062	0.00042
L3	0.00224	0.00062	68 nH	0.00397
L4	0.00012	0.00042	0.00397	19.3 nH

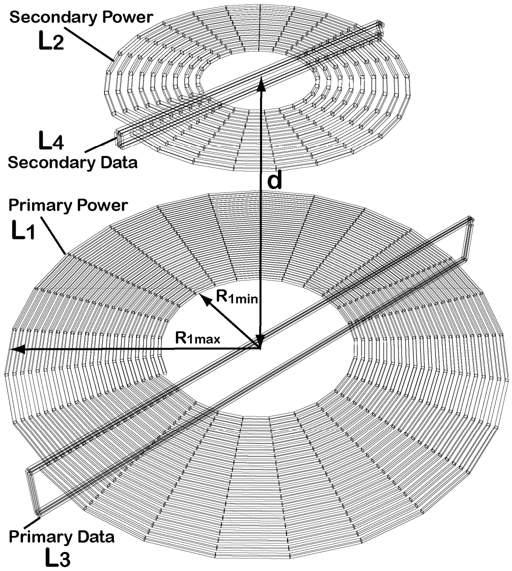

Fig. 5. Three Dimensional rendering of the forward data and power transmission coils

internal data coils, is approximately 33 times smaller than k_{34}, the direct coupling between the external and internal data coils, which can greatly help in reducing the interference.

IV. Simulation Results

To evaluate the interference between power and forward data carriers, circuit simulations were performed with the inductive wireless link LC-tank circuits, shown in Fig. 1, using coils parameters of Table 1. Power is transmitted at f_P = 125 kHz using stagger tuning [11]. FSK modulation is used to transmit data at high rate using f_{FD} = 25/50 MHz carrier as explained in [6]. The transient and frequency responses of the inductive wireless link in Fig. 6 show the insignificant effect of the power carrier interference with the received FSK data carrier, which is the result of proper coil design, large carrier frequency separation, and band-pass filtering effect of the tuned LC-tanks. Further high-pass filtering can be provided on-chip, as shown in Fig. 1, if needed.

V. Conclusions

A new approach for wireless efficient power and wideband bidirectional data transmission to implantable biomedical devices is presented, using three different carrier frequencies. Coupling coefficients between coils with various geometries are modeled and design guidelines are deducted as how to maximize or minimize them. Two pairs of coils for power and forward data transmission are designed with maximum direct coupling within each pair and minimum cross coupling between the two pairs. This is to improve power efficiency and reduce interference between carriers.

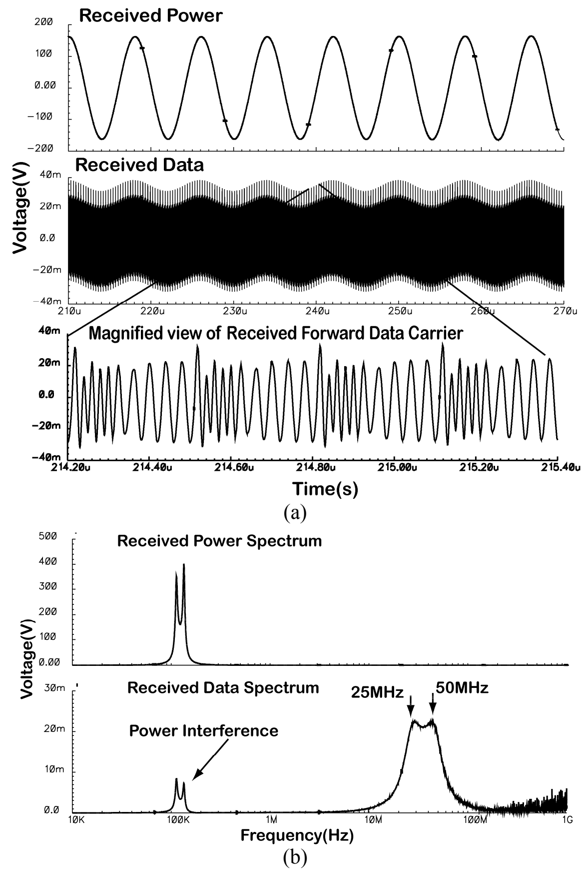

Fig. 6. (a) Transient and (b) frequency responses of the inductive wireless link showing the attenuated power carrier interference with the received FSK data carrier as a result of the measures explained in this paper.

References

[1] B. Smith *et al.*, "An externally powered, multichannel, implantable stimulator-telemeter for control of paralyzed muscle," *IEEE Trans. Biomed. Eng.*, no. 4, pp. 463-475, Apr. 1998.

[2] W. Liu *et al.*, "A neuro-stimulus chip with telemetry unit for retinal prosthetic device," *IEEE J. Solid-State Cir.*, vol. 35, pp. 1487-1497, Oct. 2000.

[3] G.J. Suaning and N.H. Lovell, "CMOS neuro-stimulation ASIC with 100 channels, scalable output, and bidirectional radio-freq. telemetry", *IEEE Trans. Biomed. Eng.*, vol. 48, pp. 248-260, Feb. 2001.

[4] IEEE standard for safety levels with respect to human exposure to radio frequency electromagnetic fields, 3 kHz to 300 GHz, 1999.

[5] R.A. Normann, E.M. Maynard, P.J. Rousche, and D.J. Warren, "A neural interface for a cortical vision prosthesis," *Vision Research*, vol. 39, pp. 2577-2587, 1999.

[6] M. Ghovanloo and K. Najafi, "A Wideband Frequency-Shift Keying Wireless Link for Inductively Powered Biomedical Implants", *IEEE Trans. Circ. Sys.* I, vol. 51, no. 12, Dec. 2004.

[7] K. Gosalia, G. Lazzi, and M. Humayun, "Investigation of a microwave data telemetry link for a retinal prosthesis", *IEEE Trans. Microwave Theory Tech.*, vol. 52, no. 8, pp. 1925-1933, Aug. 2004.

[8] C.M. Zierhofer and E.S. Hochmair, "Geometric approach for coupling enhancement of magnetically coupled coils", *IEEE Trans. Biomed. Eng.*, vol. 43 , no. 7, pp. 708 – 714, July 1996.

[9] FastHenry2 available at: http://www.fastfieldsolvers.com/

[10] C.M. Zierhofer and E.S. Hochmair, "High-efficiency coupling-insensitive transcutaneous power and data transmission via an inductive link," *IEEE Trans. Biomed. Eng.*, vol. 37, pp. 716–722, July 1990.

[11] D. G. Galbraith, M. Soma, and R. L. White, "A wide-band efficient inductive transdermal power and data link with coupling insensitive gain," *IEEE Trans. Biomed. Eng.*, vol. 34, pp. 265–275, Apr. 1987.